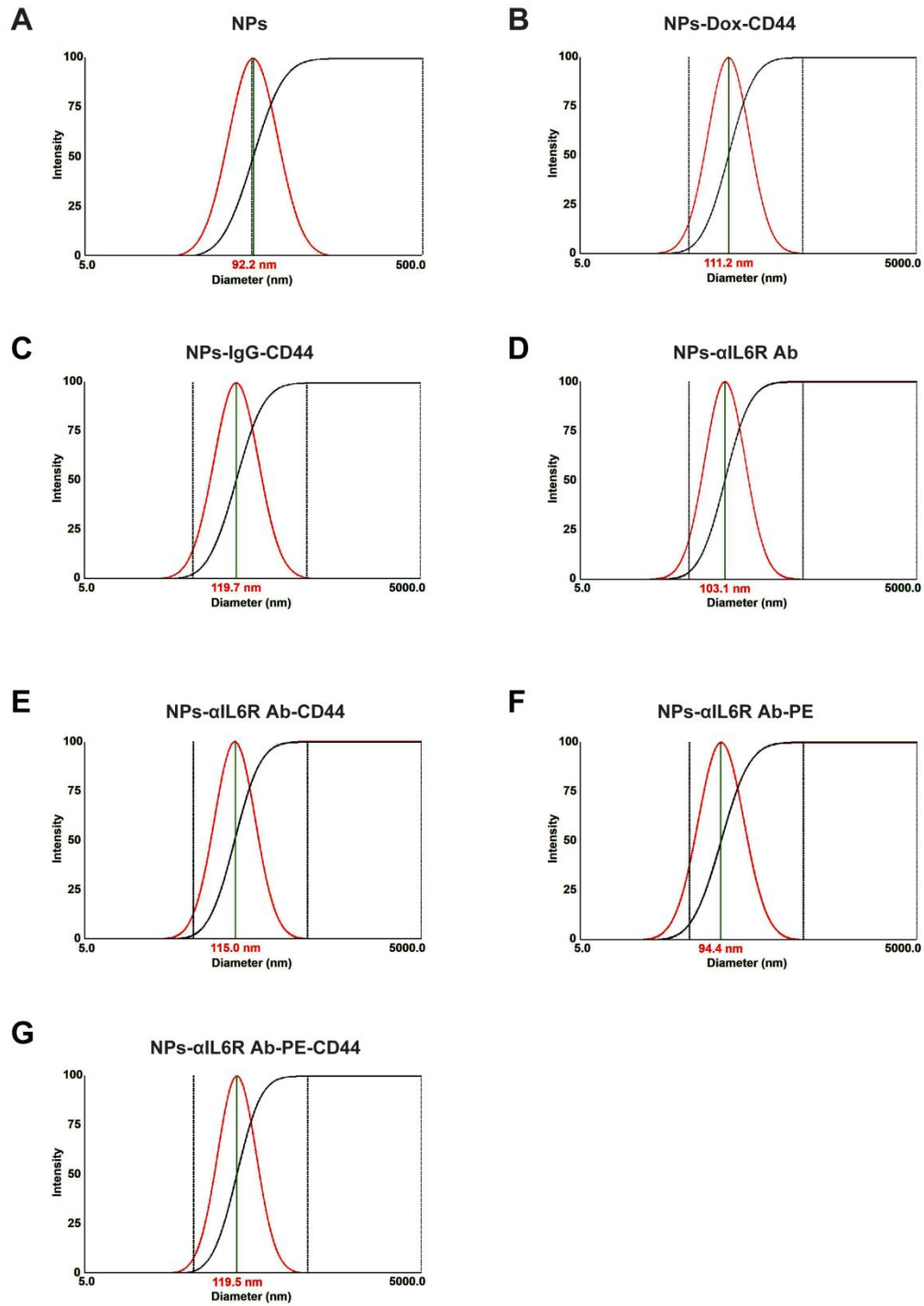
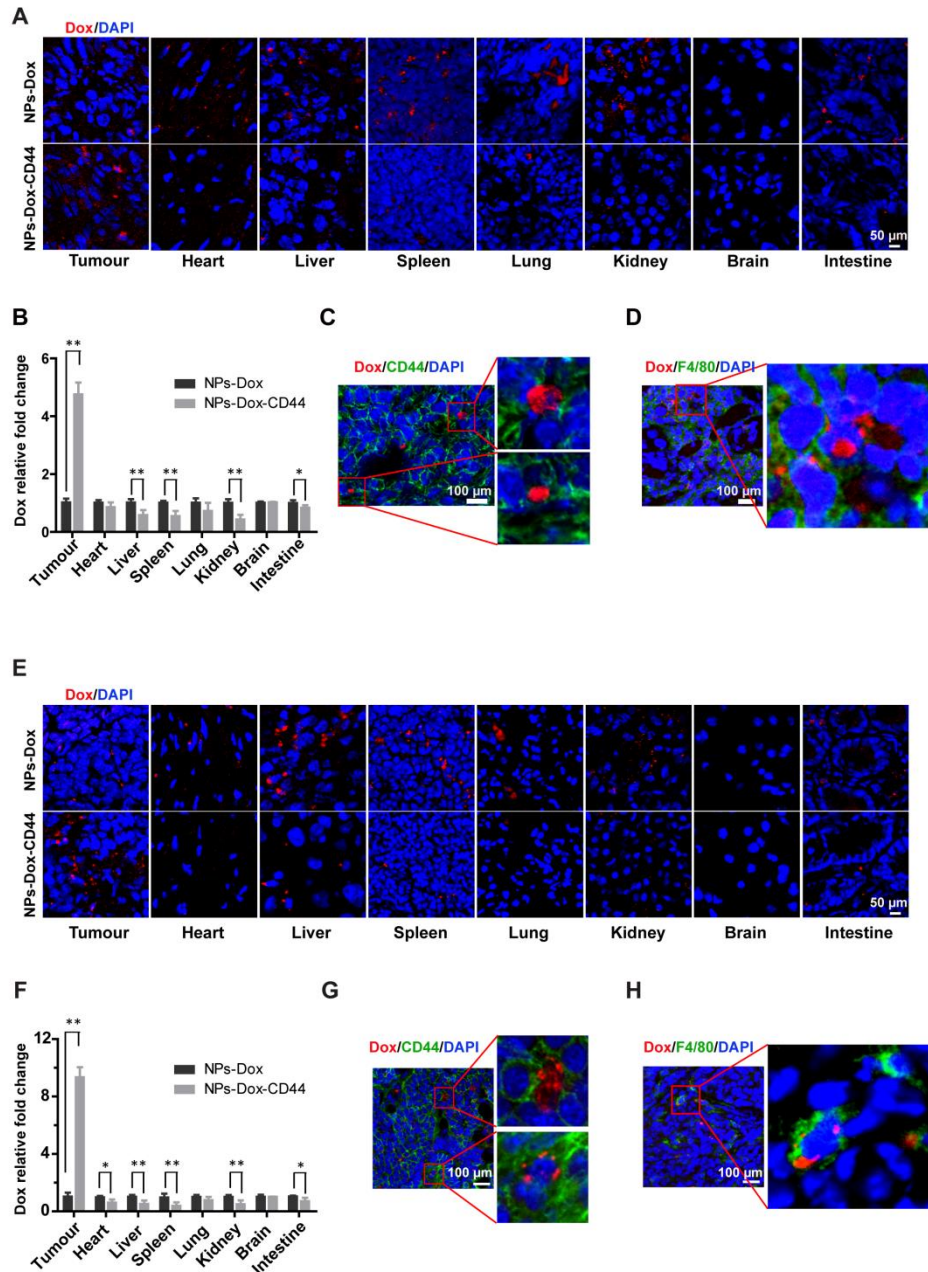


## Supplementary Information



**Figure S1.** Representative dynamic light scattering (DLS) measurements for different nanoparticles.



**Figure S2.** Increased targeting efficiency of CD44 targeted liposomal nanoparticles in breast tumour tissues. **A.** Confocal images of Dox in various tissues of BALB/c mice bearing 4T1 xenografts that were treated with NPs-Dox or NPs-Dox-CD44 for 4 hs. **B.** The relative fold changes for the concentration of Dox in various tissues of BALB/c mice treated with NPs-Dox-CD44 when compared with the NPs-Dox treatment control. Data were presented as the mean + SD,  $n = 6$  mice. The representative images showing the distribution of CD44 and Dox (**C**), F4/80 and Dox (**D**) in tumour xenografts of BALB/c mice. **E.** Confocal images of Dox in various tissues of MMTV-PyMT mice. **F.** The relative fold changes for the concentration of Dox in various tissues of MMTV-PyMT mice treated with NPs-Dox-CD44 when compared with the NPs-Dox treatment control. Data were presented as the mean + SD,  $n = 6$  mice. The representative images showing the distribution of CD44 and Dox (**G**), F4/80 and Dox (**H**) in breast tumours of MMTV-PyMT mice.

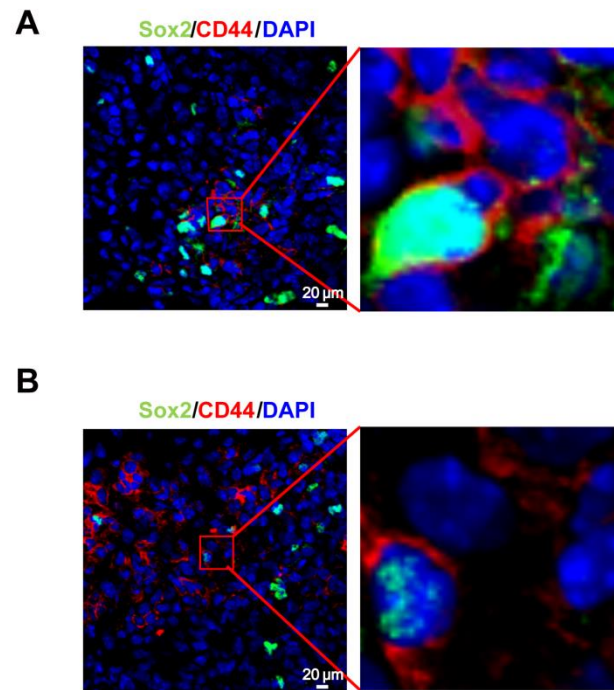


**Figure S3.** Immunofluorescence images of Sox2 (green) and CD44 (red) in 4T1 tumour xenograft of BALB/c mouse (**A**) and primary tumour tissue of MMTV-PyMT mouse (**B**).

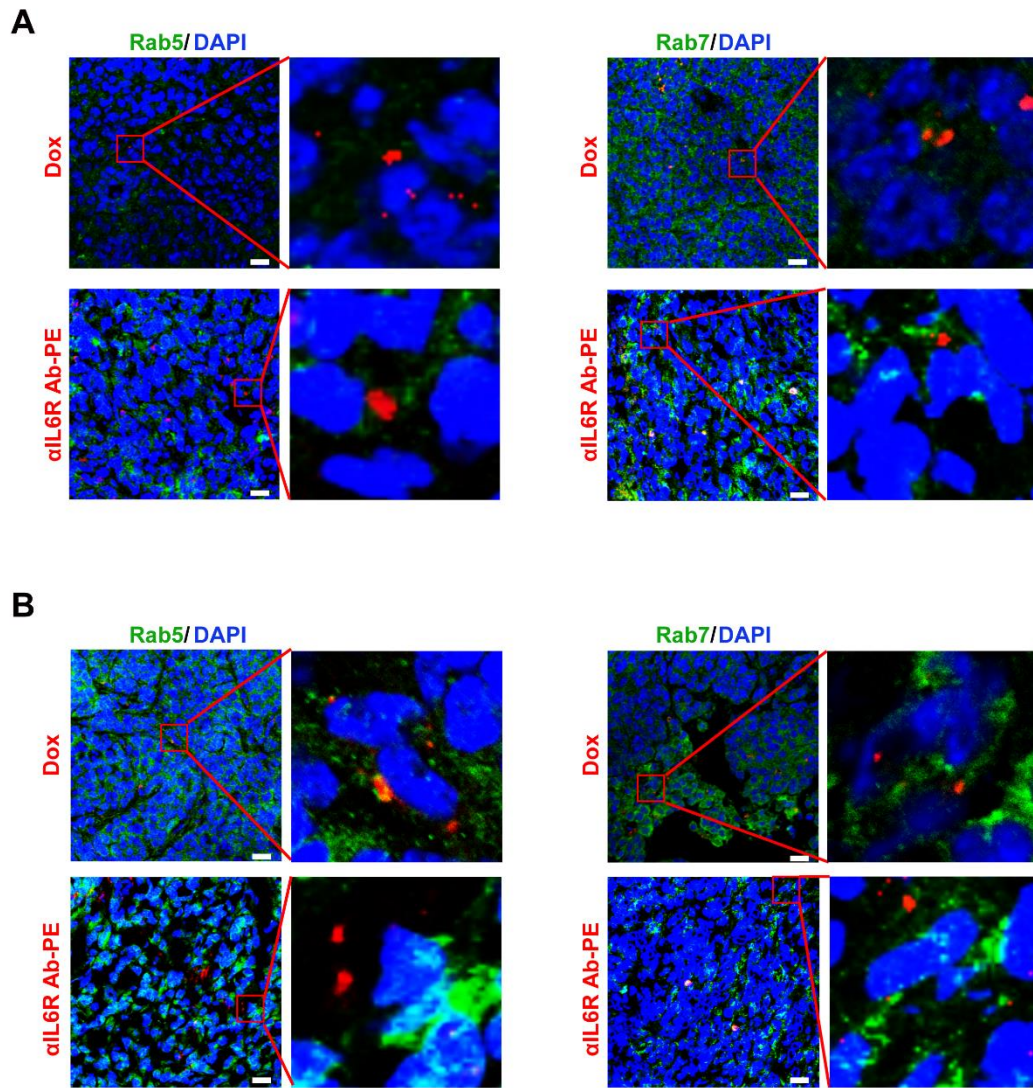


**Figure S4.** Representative immunofluorescent images of Rab5 (green) or Rab7 (green) with Dox (red) or  $\alpha$ IL6R Ab-PE (red), in 4T1 tumour xenografts of BALB/c mice (A) and primary tumour tissue of MMTV-PyMT mice (B) that were treated with NPs-Dox-CD44 for 4 hs or NPs- $\alpha$ IL6R-PE-CD44 for 6 hs, scale bar: 40  $\mu$ m.